Supplementary Material: 3D Flow Field Estimation around a Vehicle Using Convolutional Neural Networks

Fangge Chen
fanggechen@mail.nissan.co.jp
Nissan Research Center, Mobility & AI Laboratory
Nissan Motor Co., LTD.
Kanagawa, Japan

Kei Akasaka
kei-akasaka@mail.nissan.co.jp
Integrated CAE and PLM Department, Aerodynamics CAE Group
Nissan Motor Co., LTD.
Kanagawa, Japan

1 Geometric Information of Dataset

A Cartesian space whose size of length(L) $\times$ width(W) $\times$ height(H) is $10m \times 4m \times 3m$ is selected to locate the vehicle shape data. The vehicle is placed on the ground of this symmetrically about the L axis. Then, the front of the vehicle is put at the length of 2 meters, which is shown in Fig. 1. Unsigned distance functions and flow fields in the space are collected in the dataset. Likewise, our task is to estimate the flow fields in this specified space.

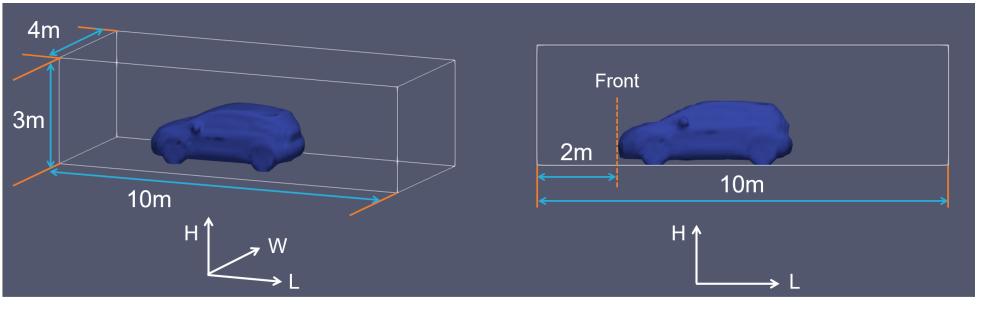

Figure 1: The selected Cartesian space and the location of vehicle.

2 Architecture Details

Details of the estimation model architecture are shown in the Fig. 2. For simplicity, the rectangle with same colour means the same layer.

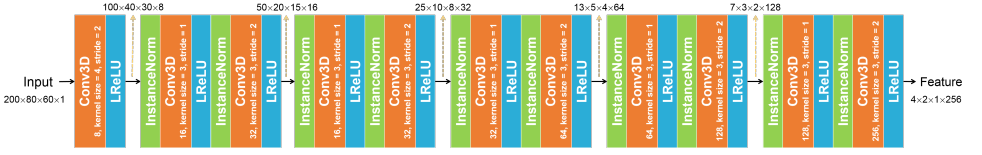

(a) Encoder

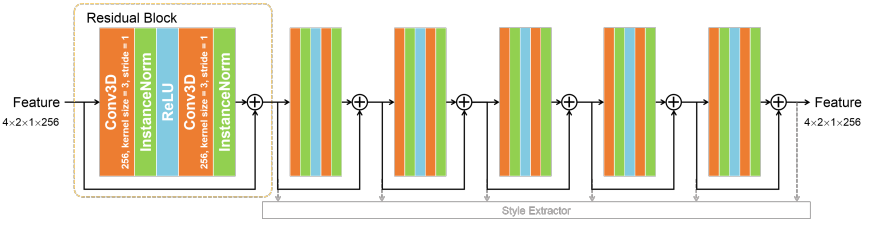

(b) Residual blocks

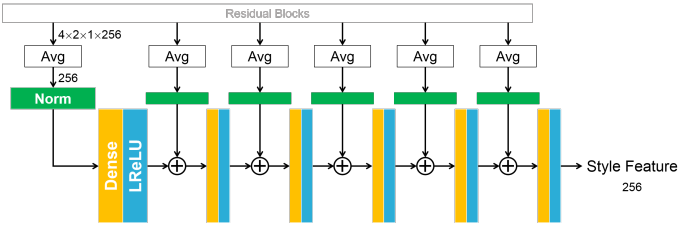

(c) Style extractor

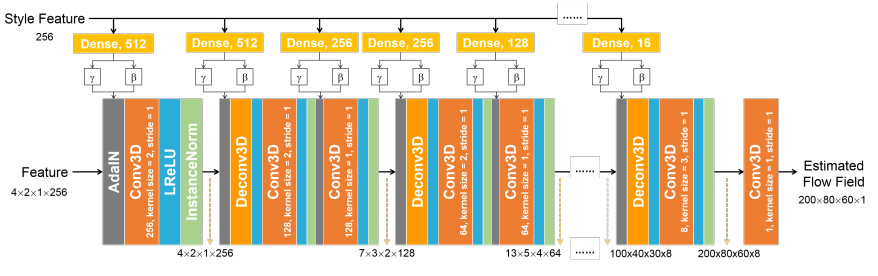

(d) Generator for a component of flow fields

Figure 2: Details of the estimation model architecture.

3 Detail Architectures used for Comparison

Two estimation models based on previous studies [10] and [12] were reimplemented for comparing with the proposed estimation model. However, because these models were designed for 2D flow field estimation from 2D shape data such as image, we revised them to fit our data size and to support 3D data training. Here, the detail architectures of these models are presented.

Fig. 3 shows the detail architecture of the estimation model based on [10] which is divided into a convolution encoding part and a convolution decoding part. Signed distance function (SDF) of the vehicle shape data is used as input of the estimation model. Here, we do the same preprocessing including mean removal and scaled by 0.01. The convolution encoding part firstly extracts a 1024-dimensional feature from SDF input. Next, in convolution decoding part, the feature is sent into 4 same generators to generate 3 components of velocity field and pressure field. Following the description in [10], we train the estimation model using a mean squared error which only calculated on where air can pass through as the loss function and RMSProp optimiser with a batch size of 64 to optimise the parameters. The parameters are all initialized using Xavier method. The main difference is that the initial learning rate is set to 10^{-3} rather than 10^{-4} for the better convergence. The learning rate decays by multiplying 0.8 every 2,500 iterations. We train the estimation model for 1,000 epochs because of comparing the proposed method in the same training status.

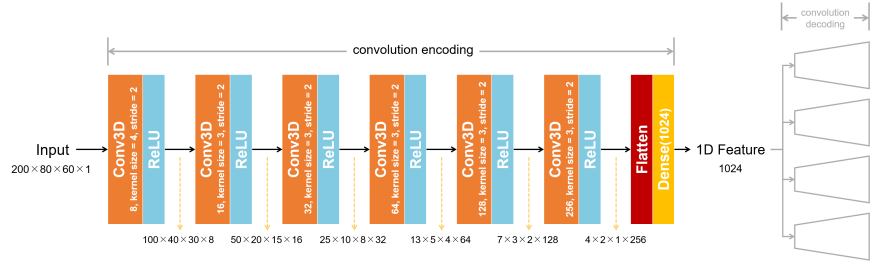

(a) Convolution encoding

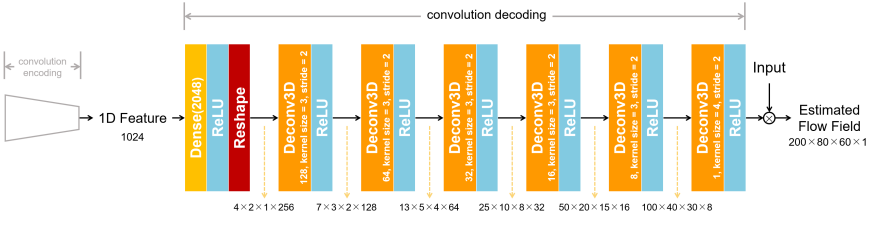

(b) Convolution decoding

Figure 3: Estimation model architecture based on [10].

Fig. 4 shows the detail architecture of the estimation model based on [12]. This is also an encoder-decoder architecture, however, all the components of flow fields are generated from a shared decoder. Although a separated decoder was proposed, the experiment showed that the shared one is more efficient. The input is SDF of vehicle shape and the output is a $200 \times 80 \times 60 \times 4$ tensor which the first 3 channels are used as velocity field and the last

channel is used as pressure field. Swish activation functions are used following all of the convolutional layers and dense layers based on description in [12]. The loss function used as follow:

$$\text{Loss}_{\text{total}} = \lambda_{\text{MSE}} \times \text{MSE} + \lambda_{\text{GS}} \times \text{GS} + \lambda_{\text{L2}} \times \text{L2}_{\text{regularization}} \tag{1}$$

where λ_{MSE}, λ_{GS}, λ_{L2} are 0.9, 0.1, 10^{-5} respectively. GS means gradient sharpening or gradient difference loss which is also a part of our loss function. We train the estimation model by setting batch size to 8 and learning rate to 10^{-4}. For the same intention, we train the estimation model for 1,000 epochs.

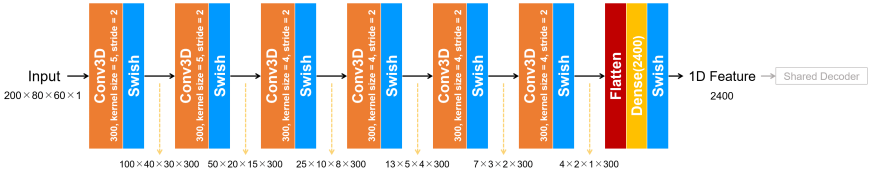

(a) Encoder

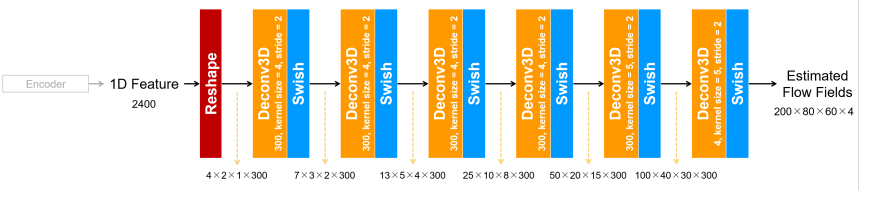

(b) Shared decoder

Figure 4: Estimation model architecture based on [12].

4 Additional Evaluation Results

The proposed method is to estimate 3D flow fields. Fig. 5 and Fig. 6 show another viewpoint of estimated velocity field magnitude and pressure field in wake region. The H × W slices at 1 meter behind the rear of the vehicles are shown in these figures. Fig. 7 shows the streamline of each vehicle, which is a 3D visualization calculated from velocity field.

Fig. 8 ~ Fig. 10 show the comparison against the previous estimation models on other cases. The results show that the proposed method improves the flow fields estimation especially in region near the vehicle surface and the wake region. In figure of differences from ground truth, we adjusted range in which all the error values can be included for observation easier. Although the differences of pressure is clear to observe, the maximum value of the range 50 Pa is 3% of the whole pressure value range. However, improving the estimation continuously is necessary because these errors also influence the aerodynamic performance of vehicle a lot.

As shown in Fig. 6 and Fig. 10, although the proposed method does the better estimation and is able to be used for rough aerodynamic performance evaluation, we found that the flow fields estimation of wake region which is behind the vehicle sometimes also does not goes well. Despite calculating and modeling the flow fields in wake region is currently also a difficult problem in aerodynamics, we will improve the estimation performance continuously by both revising the estimation model and associating with physical laws in the future.

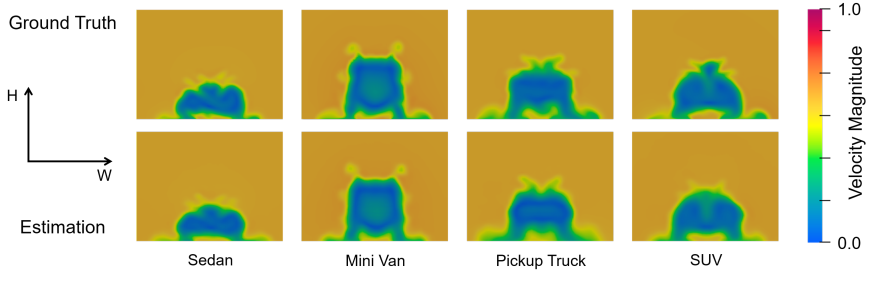

Figure 5: Estimated velocity filed from another viewpoint in wake region.

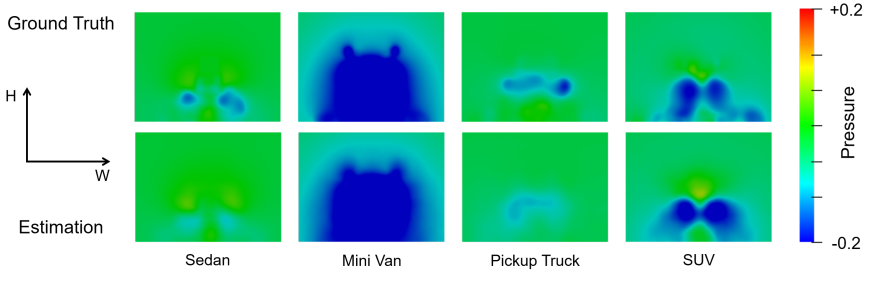

Figure 6: Estimated pressure filed from another viewpoint in wake region.

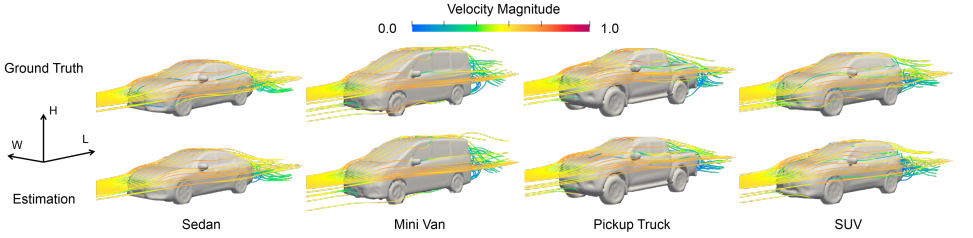

Figure 7: Streamlines of velocity fields for a 3D visualization.

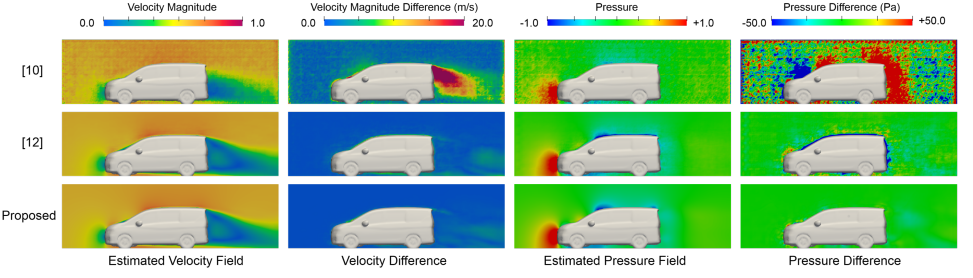

Figure 8: Comparison results of a mini van in test set.

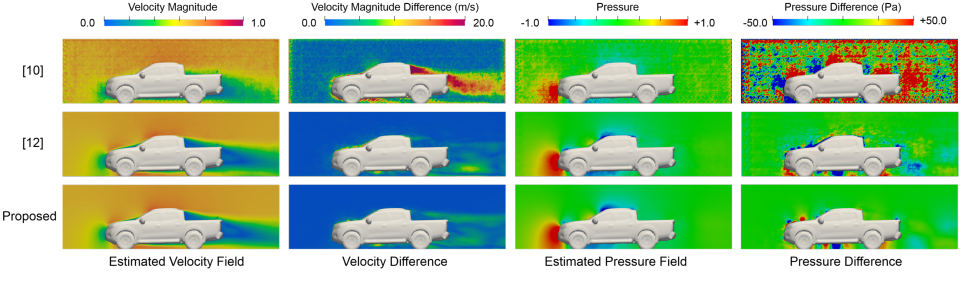

Figure 9: Comparison results of a pickup truck in test set.

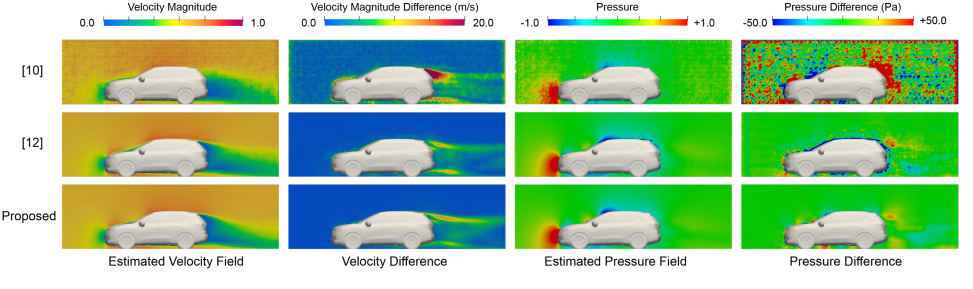

Figure 10: Comparison results of a SUV in test set.